

Machine learning regression-based RETRO-VLP for real-time and stabilized indoor positioning

Ali H. Alenezi 1 · Mahmoud Nazzal 2 · Ahmed Sawalmeh 1,3 · Abdallah Khreishah 2 · Sihua Shao 4 · Muhannad Almutiry 1

Received: 1 November 2022 / Revised: 20 November 2022 / Accepted: 28 November 2022 © The Author(s), under exclusive licence to Springer Science+Business Media, LLC, part of Springer Nature 2022

Abstract

Many real-world applications require real-time and robust positioning of Internet of Things (IoT) devices. In this context, visible light communication (VLC) is a promising approach due to its advantages in terms of high accuracy, low cost, ubiquitous infrastructure, and freedom from RF interference. Nevertheless, there is a growing need to improve positioning speed and accuracy. In this paper, we propose and prototype a VLC-based positioning solution using retroreflectors attached to the IoT device of interest. The proposed algorithm uses the retroreflected power received by multiple photodiodes to estimate the euclidean and directional coordinates of the underlying IoT device. In particular, the relative relationship between reflected light magnitude and reflected power is used as input to trainable machine learning regression models. Such models are trained to estimate the coordinates. The proposed algorithm excels in its simplicity and fast computation. It also reduces the need for sensory devices and active operation. Additionally, after regression, Kalman filtering is applied as a post-processing operation to further stabilize the obtained estimates. The proposed algorithm is shown to provide stable, accurate, and fast. This has been verified by extensive experiments performed on a prototype in real-world environments. Experiments confirm a high level of positioning accuracy and the added benefit of Kalman filtering stabilization.

Keywords VLC · Positioning · Localization · Retroreflectors · IoT · Kalman filtering stabilization

Mahmoud Nazzal mahmoud.nazzal@ieee.org

Ali H. Alenezi ali.hamdan@nbu.edu.sa

Ahmed Sawalmeh a.sawalmeh@inu.edu.jo

Abdallah Khreishah abdallah@njit.edu

Sihua Shao sihua.shao@nmt.edu

Muhannad Almutiry muhannad.almutiry@nbu.edu.sa

Published online: 31 December 2022

- Northern Border University, 73222 Arar, Saudi Arabia
- New Jersey Institute of Technology, Newark, NJ 07102, USA
- ³ Irbid National University, Irbid 21110, Jordan
- New Mexico Tech, Socorro, NM 87801, USA

1 Introduction

Accurate and timely positioning of devices, tools, and objects is gaining increasing attention in both home and industrial environments. Positioning is required in warehouse workplaces, airports, and shopping malls. As an example, it is required to keep track of robots in a warehouse delivery robot team for the purposes of collision avoidance and latency minimization. Since most Internet of Things (IoT) devices are typically used indoors, it is encouraged to use an indoor positioning approach. A traditional positioning approach is the Global Positioning System "GPS". However, it is not suitable for indoor environments and requires expensive communication and hardware overhead on the target device. A better alternative is a visible light communication (VLC) based approach [1]. The main idea behind this approach is to project light from a light source onto an object of interest and localize it using information extracted from the signal



reflected from it. Such information includes intensity, angle of incidence, polarization, and light distribution pattern. There are various VLC positioning approaches based on what information is obtained and how it is used for positioning. Visible Light Positioning (VLP) technology describes the capability of indoor positioning using visible light emitted by existing room lighting fixtures and capturing the emitted light with a receiving unit equipped with one or more light-sensitive devices [2].

Visible Light Sensing (VLS) extends visible light capabilities into the realm of sensing and detection [3]. Applications that can be handled by VLS range from simple pose recognition [4], occupancy or presence detection [5] to gesture recognition [6], amongst many more. With VLS, the object of interest reflects the light emitted by the light source back to the light-receiving element. Information can be conveyed through the placement of reflective materials or other components (such as LCD shutters) that modulate the spectrum and/or intensity of the reflected light. An LCD shutter keeps alternating between opaque and transparent states thereby allowing light passage at a controllable frequency. This is important for the identification of several devices.

The VLC-based approach possesses several attractive advantages over other solutions. First, it requires minimal [7] or even no additional hardware complexity [8]. Second, is the minimized interference in the VLC domain due to its line-of-sight (LoS) nature promising for very fine-grained positioning accuracy levels [9]. Moreover, some recent positioning approaches achieve cm-level accuracy operation [10]. Also, the usefulness of the VLC approach is more strongly motivated by the widespread of light-emitting diodes (LEDs) for illumination in home, office, and industrial environments.

Although the VLC-based approach has several advantages, it still faces certain challenges. First, is the nonconvexity of positioning when viewed as an optimization problem. This stems from the non-linear relationship between object coordinates and signal properties received by PDs. This creates a barrier to treating positioning as a standard optimization problem [11] as this solution framework tends to give local optima. Also, the signal received by the target device depends on both its position and orientation. This makes accurate positioning in terms of coordinates and angles a more challenging problem.

1.1 Motivation and related work

Non-VLP positioning approaches include RF-based methods. This category includes FRID, Bluetooth, WiFi [12]. However, these positioning methods have accuracy levels in the order of 1 m, whereas ultra-wideband (UWB)-based positioning can achieve positioning accuracies within 10

cm. Still, this technique has the drawbacks of high hardware cost, short battery life, and lack of interaction with current devices. Clearly, some of these drawbacks are eliminated by using the VLC solution.

Traditional VLP approaches are based on exploiting the geometric relationship between the device of interest and an intense light source [13]. Despite their simplicity, these approaches require some knowledge of the target device. Partial or complete directional information, the known altitude of the user equipment (UE), or the complete alignment of the transmitter and UE directions [11]. Another category of VLP approaches is based on optimization. In this setting, the positioning problem is formulated as a standard optimization formulation and the goal is to optimize the positioning accuracy. Attempts in this direction include gradient descent, linear search, and Newton's method [14]. This approach reduces the need for prior knowledge of the object of interest required by conventional methods. However, the non-convexity of the problem limits the results to local optima. As a result, this approach tends to degrade positioning performance, depending on the quality of the local solution obtained. The third category is based on sparse coding, exploiting the sparsity of the solution to guide optimization searches. However, there are still challenges associated with extracting the correct sparsity of the solution. This requires both using the correct sparsity degree and identifying the actual areas where the solution is sparse. Both of these requirements are important and require further research for this approach to be effective in a variety of operational situations.

A recent study, RETRO [10], uses an LCD shutter to set up a real-time reverse VLC channel by modulating retroreflected light from a corner-cube retroreflector. A retroreflector is a small device that can reflect light from the VLC back to the light source with minimal scattering, minimizing errors in estimating the received power. This setup allows for identifying an IoT device using LCD shutters with different operating frequencies. In terms of performance, RETRO offers centimeter-level precision and accuracy.

An optical retroreflector (RR) is a device that, unlike a mirror, reflects the incident light towards the direction of the source, with minimal scattering. RRs can be implemented with different technologies and are used in many fields, including free-space optical and satellite communications. Cheap RR materials are commonly available and are used for road signs, bicycles, and clothing for road safety. A popular type of RR is the corner-cube retroreflector (CCRR) [15], which is composed of three mirrors arranged into a 90-degree corner geometry. Regardless of the relative orientation of the direction of the incident



beam, the ray will be reflected in the source after three reflections, as pictorially shown in Fig. 1.

An extension of RETRO is PassiveRETRO [16], where retroflectors are completely passive. Subsequently, our previous work [17] exploits the relative relationships between the magnitudes of reflected light ray power to estimate the euclidean coordinates. This is achieved by formulating a direct mapping between the power magnitudes and each coordinate. However, that work does not offer to estimate the angular coordinates, and is, by design, restricted to positioning in a limited area under the light source.

Another line of research [18] explores the use of commercially available retroreflective foils for VLC-based positioning. It is based on the idea that light strikes a retroreflective sheeting toward a photosensitive device placed close to the light source. In this line, [19] achieves high positioning accuracy at the expense of high computation and excessive memory requirements. Subsequently, [18, 20] point out that a random forest supervised ML approach is suitable for the VLC positioning problem, while at the same time having significant advantages in computational complexity and memory requirements. However, this approach still lacks high-precision and real-time positioning.

1.2 Contributions and organization

Based on the above, our motivation is to improve positioning accuracy while maintaining real-time performance. Below is a summary of the contributions featured in this paper.

 Regression models for estimating the coordinates of IoT devices based on reflected VLC power: sensed at a few

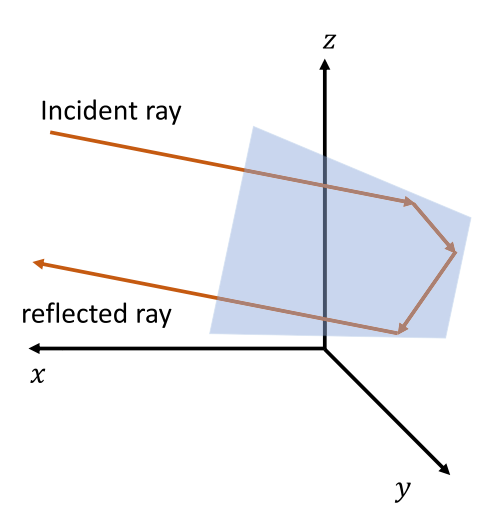


Fig. 1 The working principle of a CCRR; reflecting light to the direction of its incidence with minimized scattering

- photodiodes (PD)s. These power measurements are quantified and used to estimate the euclidean and angular coordinates of the object through trainable regression models. Such models are trained to capture the correspondence between the coordinates and the magnitudes of power received by the PDs
- Using a Kalman filtering process as a stabilization aid for estimated coordinates: Rather than depending solely on the outcomes of regression models, a Kalman filtering stage [21] helps reduce abrupt jumps in the outputs and leads to more stable estimates by incorporating noise suppression in the measurements.
- Prototyping the proposed algorithm on a real-world testbed: used to test the operation in real scenarios.
 With this testbed, extensive performance evaluation experiments are conducted to examine its accuracy and time complexity.

1.2.1 Notation

Lower-case plain-faced, lower-case bold-faced, and uppercase bold-faced letters represent scalars, vectors, and matrices, respectively. In a matrix X, the symbol x_i denotes its i- th column. The symbol x_i means the realization of a variable x at time slot t.

1.2.2 Organization

The remainder of this paper is organized as follows. Section 2 presents the system model and revises the preliminaries. The proposed positioning algorithm is presented in Sect. 3. Section 4 details the prototyping and experimentation of a proof of concept of the proposed algorithm, with the conclusions in Sect. 5.

2 System model and preliminaries

2.1 System model

We adopt a system model similar to the one in [10]. As shown in Fig. 2, the goal is to obtain estimates of the

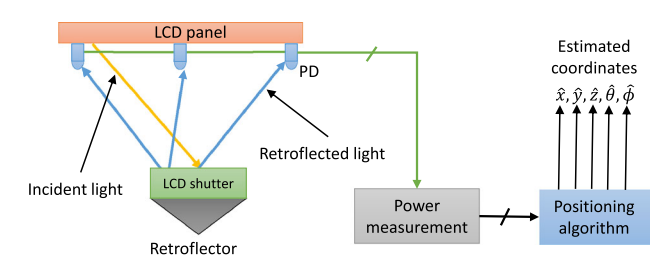


Fig. 2 The main components of the system model



coordinates of the retroreflector's euclidean $(\hat{x}, \hat{y}, \text{ and } \hat{z})$ and angular coordinates (the evaluation angle $\hat{\theta}$ and the azimuth angle $\hat{\phi}$). To achieve this goal, this model consists of the following components: First is an LED panel that acts as a (powerful) light source. It is noted that this setting applies to any available standard light source in a home or industrial outdoor environment. The second is a retroreflector circuit consisting of a retroreflector covered by an LCD shutter whose closing frequency is controlled. We especially use a corner cube retroreflector. This is a setting where the device of interest passively reflects VLC power and the positioning is done by the source device. Shutters allow or deny the passage of light by alternating between opaque and transparent states at a controllable frequency. To do this, the retroreflector reflects the incident beam into a parallel reflected beam, which is received by the PD. However, we need to measure this waveform at a specific shutter frequency. This way one can position multiple devices at the same time. To this end, the position of the device determines the power received by the PD. Therefore, position coordinates can be estimated using the correspondence between position and power. Those PDs are placed to uniformly sample the LCD panel as pictorially represented in Fig. 3. Also, the five coordinates x, y, z, θ , and ϕ are illustrated by Fig. 4. Fundamentally, the unknowns in this system are the five coordinates. Thus, it is sound to think of using five PDs as five sources of information.

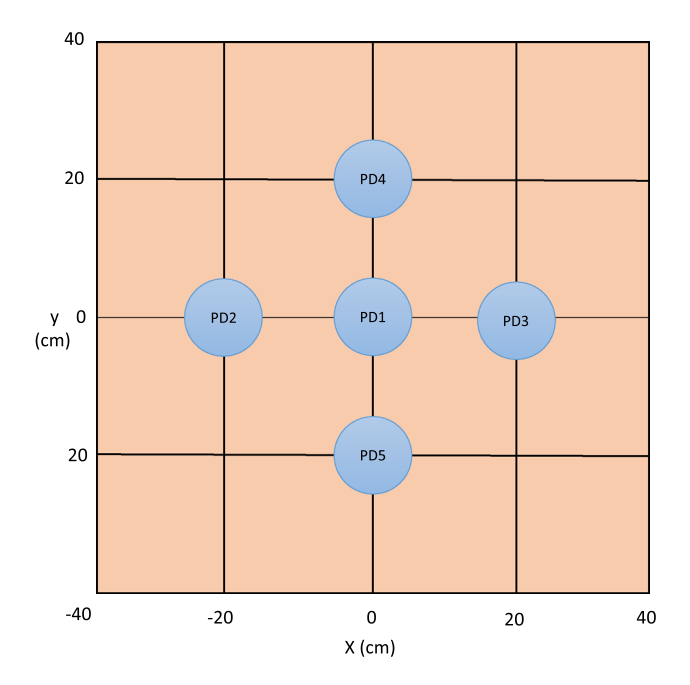


Fig. 3 A top view of the system showing the PD placement on the light source



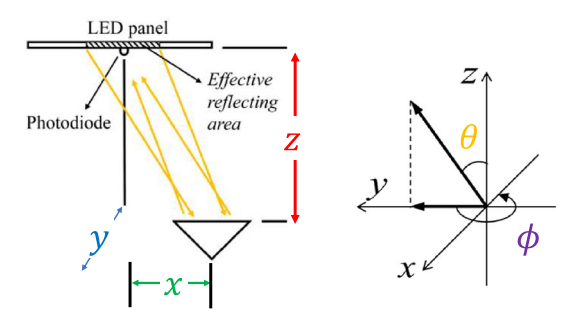


Fig. 4 An illustration of the euclidean coordinates x, y, and z and the elevation and azimuth angles θ , ϕ , respectively

2.2 Support vector machine regression

Regression can be cast as minimizing the sum of squared errors between ground-truth values and the corresponding estimates. It is thus a least squares estimation and can be viewed as follows.

$$\min \sum_{i=1}^{m} (y_i - \hat{y}_i)^2 = \sum_{i=1}^{m} (y_i - (\mathbf{w} \cdot \mathbf{x}_i + b))^2$$
 (1)

where $\hat{y_i}$ is the estimate of the true label y_i which can be given by

$$f(x) = w\Phi(x) + b \tag{2}$$

where $\Phi(x)$ is a higher-dimensional feature space, w is a weight vector, and b is a threshold. w and b can be estimated by minimizing the following regularized risk function.

$$R(C) = C \frac{1}{n} \sum_{i=1}^{n} L(d_i, y_i) + \frac{1}{2} ||w||^2$$
(3)

where C is a penalty parameter of error, d_i is the desired value, n is the number of observations, and the summation models the empirical error. This represents the parameter optimization during the iterations of the training process. The Support Vector Machine (SVM) algorithm [22] is a leading regression technique to find the estimated outcomes of given inputs.

When a given dataset cannot be linearly handled, one can transform it into a high dimensional feature space using a nonlinear mapping $\varphi(x)$, where we can carry out the linear regression despite the nonlinearity of the data. By defining the kernel function of the inner product of the high dimension feature space $K(x_i, y_i) = \varphi(x_i)\varphi(y_i)$, the inner product of a variable in the high dimension space can be obtained by operating in the original space through the kernel function.

$$\min \left\{ \frac{1}{2} \sum_{i,j=1}^{l} (a_i^* - a_i) \left(a_j^* - a_j \right) K(x_i \cdot x_j) \right.$$

$$\left. + \varepsilon \sum_{i}^{l} (a_i^* + a_i) - \sum_{i}^{l} y_i (a_i^* - a_i) \right\}$$

$$\text{s.t. } \sum_{i}^{l} (a_i - a_i^*) = 0$$

$$0 \le a_i, \quad a_i^* \le C, \quad i = 1, \dots, l$$

$$(4)$$

where a is dual variable for each data point and ϵ is an error threshold. Eventually, the regression decision function is obtained as follows.

$$f(x) = \sum_{i=1} (a_i - a_i^*) K(x_i \cdot x) + b$$
 (5)

where b is disclosed in (2).

3 Regression models for estimating coordinates based on reflected power observation

3.1 Machine learning regression for estimating the coordinates

According to the free space optical path loss, one may model the received optical power as follows [10].

$$P_r = P_t \frac{(ml+1)A_s}{8\pi d^2} \cos^{ml+1} \gamma \alpha \tag{6}$$

where P_t is the transmitted optical power multiplied by reflector loss (reflector loss includes the transmission loss of the coating material and the reflection loss of each reflection surface), m is the Lambertian index, A_S is the effective sensing area of PD, d is the distance between the PD and the retroreflector, γ is the radiance angle, and α is the ratio of the effective reflecting area to the maximum effective reflecting area.

Based on the discussion above, the magnitude of received PD power is directly correlated to how close the retroreflector is. To verify this assumption, Fig. 6 shows the power received from five PDs when the retroreflector is placed 100 cm directly below PD1. The power received on PD1 is the highest among all PDs. This implies a clear correspondence between the coordinates of the retroreflector's position and the relative relationship between the PD powers. This suggests that one can train a machine-learning model to extract and exploit this correspondence.

A regression model can be used to exploit the relationship between received power and coordinates. Therefore, we propose to use 5 regression models, one for each

coordinate. That is the Euclidean angular coordinates of x, y, z, θ , and ϕ . Different models are needed since operation scenarios are different. In particular, the power variation pattern with respect to distance is not the same for the three coordinates. Thus, we need a separate model for each coordinate. Figure 5 shows a block diagram description of the proposed estimation. Each model is trained separately on a specific data set of performance measures and respective ground truth coordinates.

A training set can be obtained by setting the object of interest at known coordinates and angular positions, measuring the power levels received from the five PDs, and recording this as an example training point. By providing such a set of training points, the trained model is expected to generalize well to unforeseen coordinates and produce accurate estimates of the corresponding coordinates. One of the key advantages of machine learning models is their generalization capabilities allowing them to well-adjust to unforeseen data. Thus, it can be assumed that if the same hardware and light sources are used, then there is no need for model retraining as the system is moved from one location to another. One needs only to retrain it if the characteristics of the received reflected power magnitudes change drastically. Besides, one can easily test the accuracy of the positioning algorithm by considering a few sample cases. Therefore, using ML regression in this application relies on two main advantages over traditional optimization techniques. First, the estimation accuracy is due to the generalizability of the ML model. Second is fast estimation due to the simple computations required for ML inference.

3.2 Kalman filtering for stabilization

A common drawback of ML models is their direct dependence on data. Here, the regression model applied to estimate the coordinates is prone to erratic behavior if the measurements provided are perturbed. Therefore, using a Kalman filtering stage promises more stable results. In particular, the Kalman filter obtains estimates based on contributions from both the ML model results and previous estimates. This effectively prevents abrupt and random changes in the estimation process. The importance of this stabilization is particularly seen in the real-time estimation of dynamically moving object coordinates.

Suppose an object of interest moves in time slots of equal length, the interval between successive positioning instances at time t and time t + 1. Let D_t denote one state of coordinates at time t. The corresponding dynamic model can be expressed as:



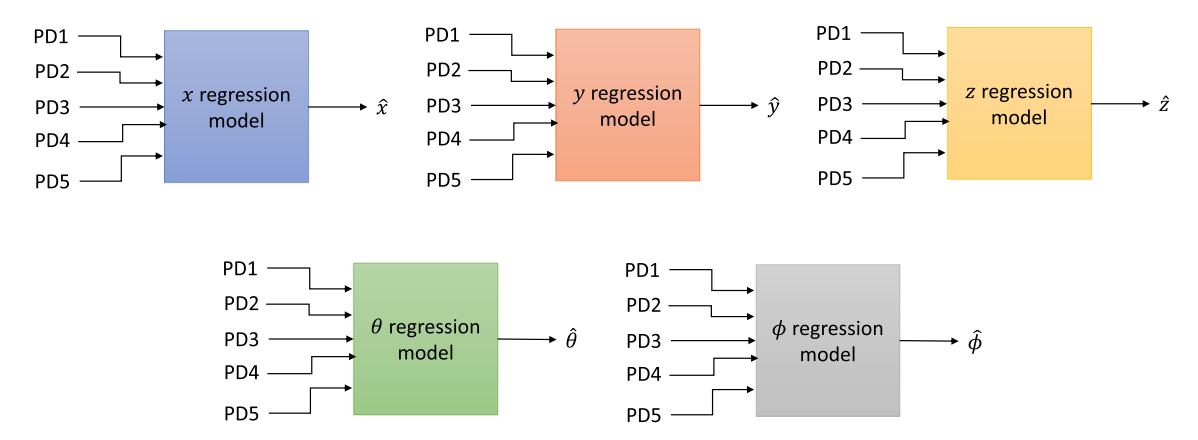


Fig. 5 Estimating the coordinates through the respective regression models

$$D_{t+1} = FD_t + B(v_t + w_t), (7)$$

where F is the state transition matrix and B is the control matrix applied to the discrete process D_t . The external uncertainty is modeled as w_t , which is Gaussian noise with covariance Q and $Q = E[w_t w_t^T]$. In the proposed model, we can assume that the object's velocity v_t (that is, the first derivative of the variation of D_t) is stable between t and t+1. Therefore, one may assume F=1 and $B=\Delta t$. To refine the predictions by previous estimates, the measure of (7) is defined as

$$z_t = HD_t + n_t, \tag{8}$$

where z_t represents the observed variable, i.e. the distance traveled D_t calculated based on the results of the ML-based positioning, and H is the scale matrix for mapping the units and scales of the states. Also, H=1, because z_t is a direct observation of D_t and n_t , is the Gaussian-distributed measurement noise with covariance R.

In its operation, a Kalman filter has two phases in each time slot: updates and prediction. In the prediction phase, the prior estimates $D_{t/t-1}$ and $P_{t/t-1}$ are calculated based on the posterior estimates $D_{t-1/t-1}$ and $P_{t-1/t-1}$. In particular,

$$D_{t/t} = D_{t/t-1} + K_t (z_t - HD_{t/t-1}) P_{t/t} = P_{t/t-1} - P_{t/t-1}K_t H$$
(9)

where K_t is the Kalman gain defined by

$$K_{t} = P_{t/t-1}H^{T}(HP_{t/t-1}HT + R)^{-1}.$$
 (10)

The update formula for (9) shows the dependence of the Kalman gain K_t on the observed measurement z_t of the later estimate $D_{t/t}$ and the prediction D_t . A small measurement noise implies a small value of R. In contrast, if the external uncertainty imposed on the prediction is small, which means that the value of Q is small based on (9) and (10), one can rely on predictions derived from $D_{t/t-1}$. The variables O and R are set empirically.

Overall, the proposed algorithm is set to merge the advantages of regression-based estimation and Kalman filtering stabilization. The main steps of the proposed algorithm are outlined in Algorithm 1.

Algorithm 1 The proposed positioning algorithm

Require: Power received by the n PDs P_i , $i \in 1, n$, and trained regression models M_x , M_y , M_z , M_θ , and M_ϕ .

Ensure: Estimated coordinates of the retroflector's position.

Assign the values of the power magnitudes P_i to their location on the PD array

Set $\hat{x} \leftarrow M_x(P)$.

Set $\hat{y} \leftarrow M_y(P)$. Set $\hat{z} \leftarrow M_z(P)$.

Set $\hat{\theta} \leftarrow M_{\theta}(P)$.

Set $\hat{\phi} \leftarrow M_{\phi}(P)$.

Stabilize the estimates using Kalman filtering and previous states.

Update the Kalman filter grain.

Return $\hat{x}, \hat{y}, \hat{z}, \hat{\theta}$, and $\hat{\phi}$



4 Testbed and experiments

4.1 Testbed and setup

A testbed is built according to the system model specified in Sect. 2. A picture of this testbed is shown in Fig. 8. A retroreflector is mounted on a tripod such that one can track its position in the physical world. As a light source, we use a commercial flat LED panel with uniformly distributed light from Hyperikon (400W, 4000K, 3770 lumens). The PD used in this article is Hamamatsu S6968 [23]. Each PD is operated in the photoconductive mode to allow for estimating the received power as a voltage across a series resistor. Figure 7 shows the schematic of the received power measurement circuit. Specifically, each PD is connected in series with a 6.8 k Ω resistor, and the series circuit is reverse-biased by a 10 VDC voltage. Therefore, the power received by the PD is proportional to the resistor voltage. As a retroreflector, we use PS976 (uncoated) manufactured by Thorlabs [24].

A Measurement Computing USB-1608FS-Plus series data acquisition device (DAQ) [25] is used to measure the above-mentioned voltage voltage. The device measures the voltage corresponding to the power of five PDs in real time with a sampling frequency of 50,000 samples/s. These measurements are sent to the PD via the USB port. We then record the power measurements via MatLab and apply a fast Fourier transform (FFT) to these power readings to

Table 1 System parameters and specifications

Item	Value
Refractive index	1.51
No. of PDs	5
PD type	S6968
A_s	150 mm2
Power sampling frequency	50 kHz
retroflector	Thorlabs PS976
LCD shutter frequency	20 Hz
LCD shutter	Pi-cell
Voltage measurement device	USB-1608FS-Plus

Table 2 SVM regression model properties and values

Property	Value
Kernel	Gaussian
Data standardization	TRUE
KernelScale	Automatic
Solver	ISDA
ShrinkagePeriod	1000

extract the actual power magnitude at the LCD shutter switching frequency. An example of an FFT power spectrum is shown in Fig. 6. As can be seen from this figure,

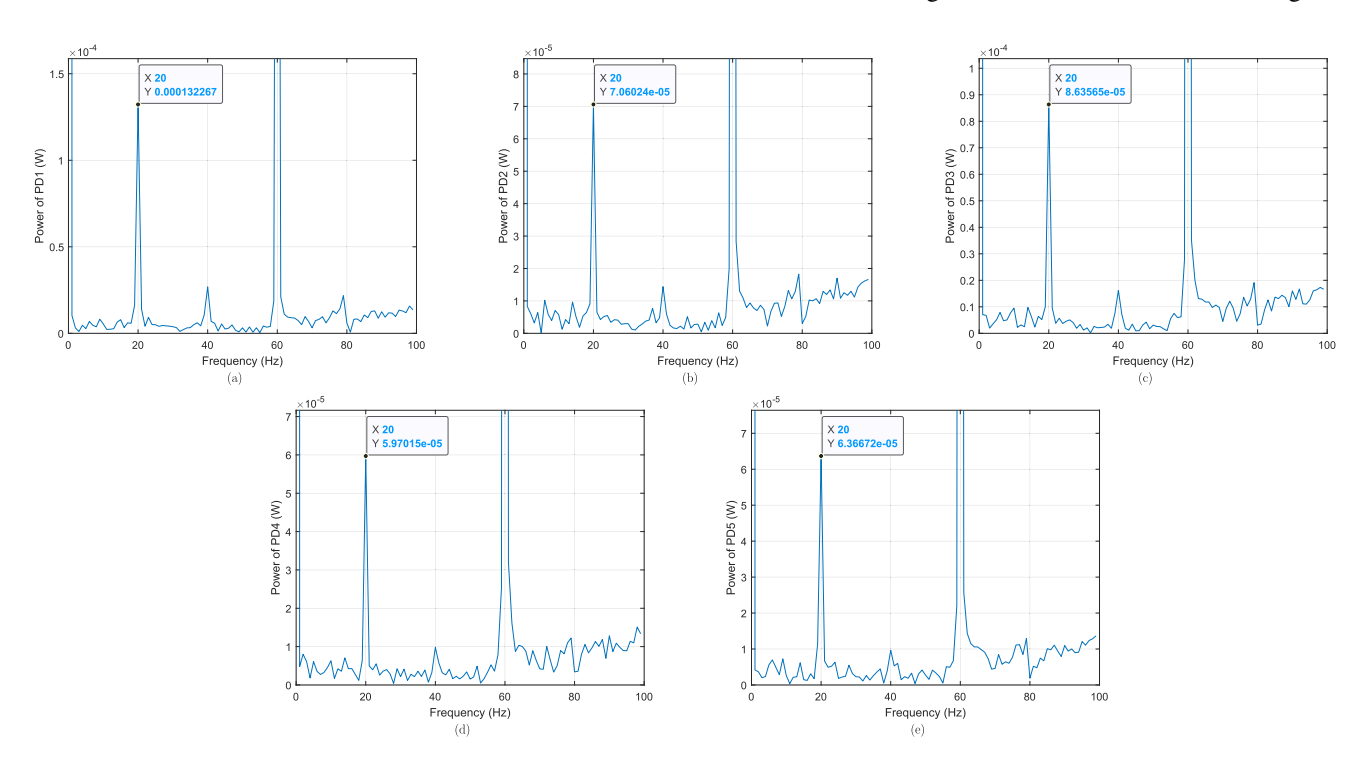


Fig. 6 Spectra of power received by PD1 through PD5 from left to right, respectively, with the retroflector placed at 100 cm underneath PD1. The power received by PD1 is larger than that received by any other PDs



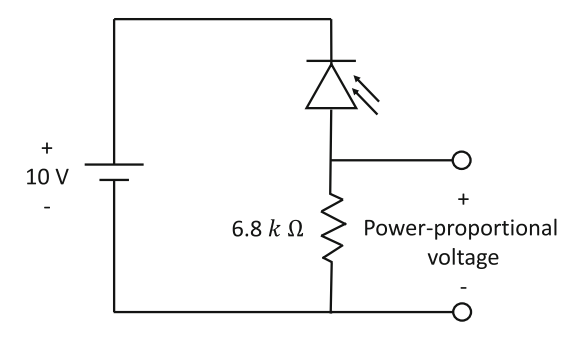
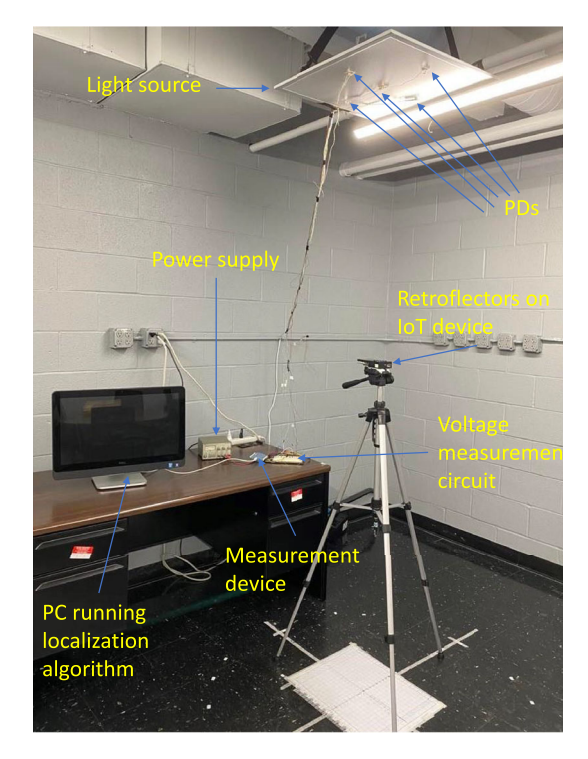


Fig. 7 PD received power measurement circuit



 $\begin{tabular}{lll} Fig. 8 A photo of the testbed used showing the main system components \\ \end{tabular}$

each spectrum has two major peaks. One at a frequency of 60 Hz because the light source operates at a dominant frequency of 60 Hz, and another small peak at 20 Hz due to power reflected from the retroreflector. There are also several other negligible peaks due to ambient noise and measurement noise.

DC power is supplied from a standard DC power supply. Finally, we perform real-time positioning on MatLab according to the steps outlined in Algorithm 1. Table 1 lists some other system parameter values.

We tested the performance of the proposed algorithm using several regression schemes. Our results show that SVM-based regression performs best among others. Therefore, we mainly present experiments based on this

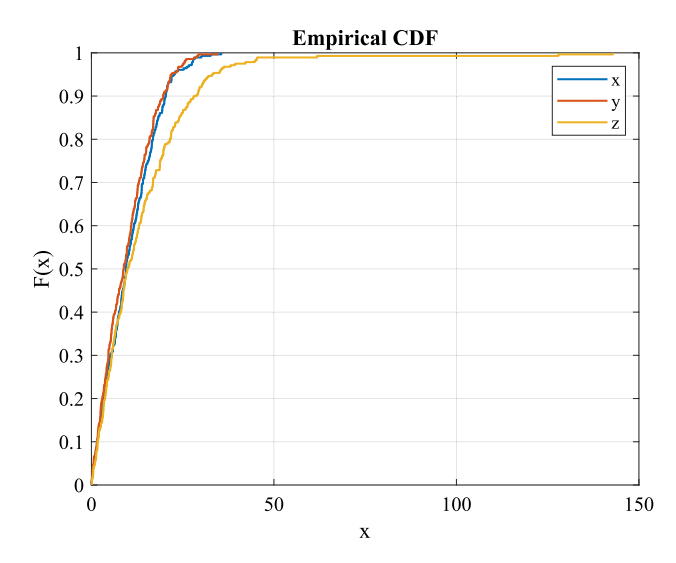


Fig. 9 Empirical CDF of positioning error for the x, y, and z coordinates

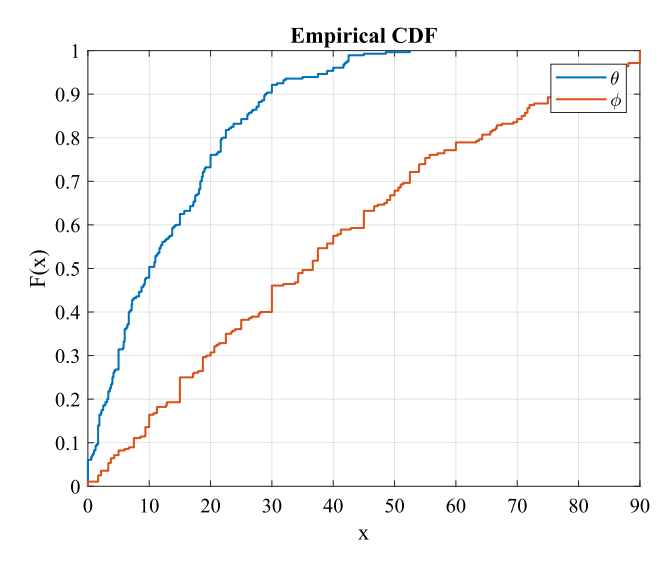


Fig. 10 Empirical CDF of positioning error for the θ and ϕ coordinates

method and do not include other experiments to avoid redundancy. Table 2 gives the specification of the SVM regression method used.

4.2 Positioning accuracy performance evaluation

In this experiment, we present a performance evaluation of the proposed algorithm. The performance metric is the empirical cumulative distribution function (CDF) of the position errors of the x, y, z, θ , and ϕ coordinates. Specifically, we place retroreflectors at known points that randomly sample the positioning system workspace. At each of these positions, we obtain estimates of the



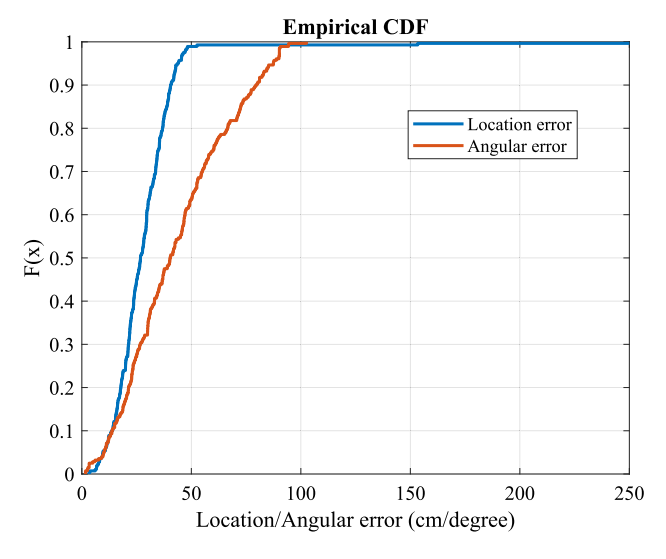


Fig. 11 Aggregate empirical CDF of positioning errors for the euclidean and angular coordinates

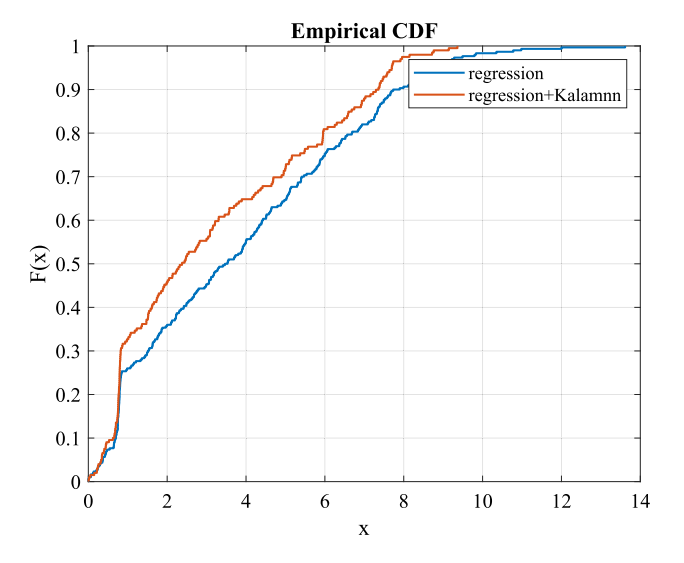


Fig. 12 The performance with and without a Kalman filtering stage

retroreflector coordinates, and between these estimates and the actual x, y, z, θ , and ϕ coordinates. Next, we calculate the absolute error of the physical world. Once the errors for all positions have been calculated, we draw an empirical CDF plot of these errors.

In this experiment, we collected measurements at 1000 data points. We then split the measurement set into training sets, testing each of the 500 mutually exclusive measurement points. Then, we trained the ML model as specified in Sect. 2. Through extensive experiments, we chose the SVM regression model for its superior performance.

Figure 9 shows empirical CDF plots of the errors in estimating the x, y, and z coordinates. A corresponding angle estimation CDF plot is shown in Fig. 10. Also,

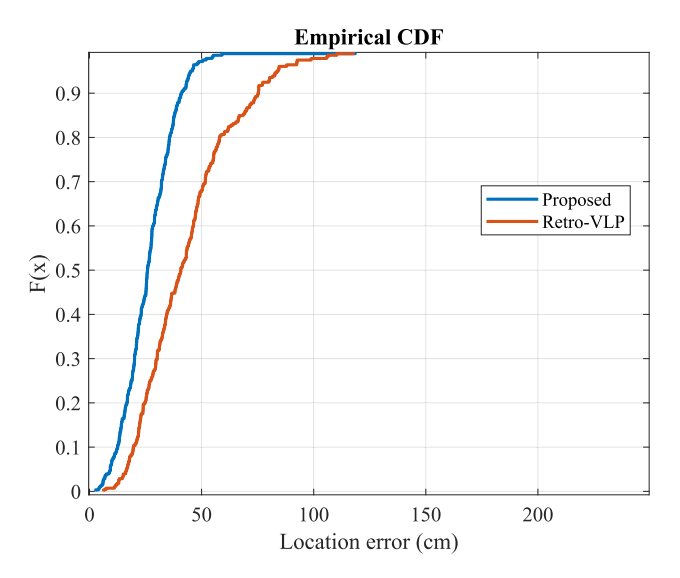


Fig. 13 Performance comparison of the proposed algorithm to the approach in [17], denoted by RETRO-VLP

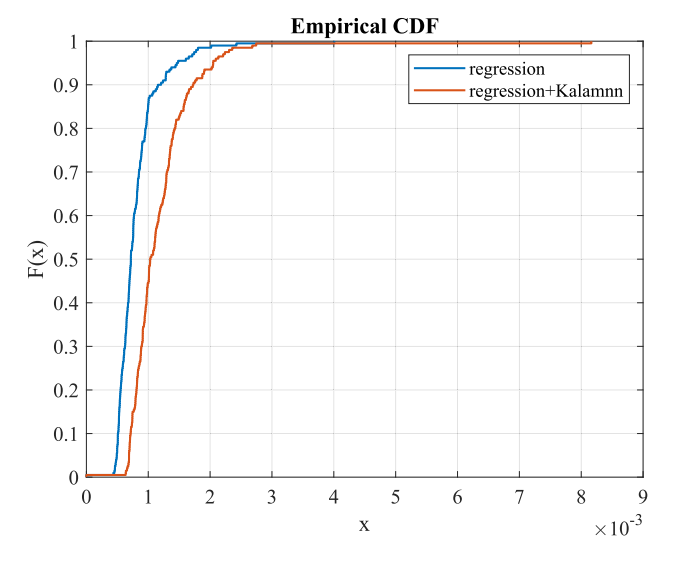


Fig. 14 A CDF plot of execution times for the regression and Kalman filtering stages of the proposed algorithm

Fig. 11 shows total error of x, y, z and angles θ and ϕ . These figures show that the proposed algorithm achieves cm-level positioning of x, y, and z. However, performance is not accurate with respect to angular coordinates.

4.3 Experimenting the Kalman filtering stabilization

To examine the added benefit of the proposed Kalman filtering stage, we conduct the following experiment. A set of measurements is obtained while the object is moving dynamically in the 3-D space. Then, starting from a known state, we use the proposed setting in Algorithm 1 to obtain



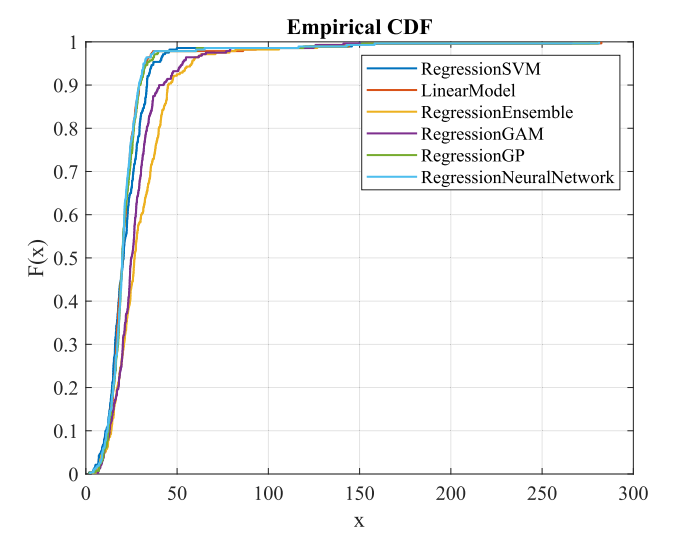


Fig. 15 Euclidean error CDF plots of positioning accuracy for several regression techniques

regulated measurements of the coordinates. Figure 12 compares the performance with and without the use of the Kalman filtering stage. This figure shows the added benefit of this filtering stage as the error is constantly smaller compared to the case where it is not used.

We compare the performance of the proposed algorithm in estimating the x, y, and z coordinates to that of our previous work in [17]. The comparison is shown in Figure 13. As can be seen, the proposed algorithm has a clear advantage over the algorithm of [17]. This awes to the use of a Klaman filtering stage and its role in estimation stabilization.

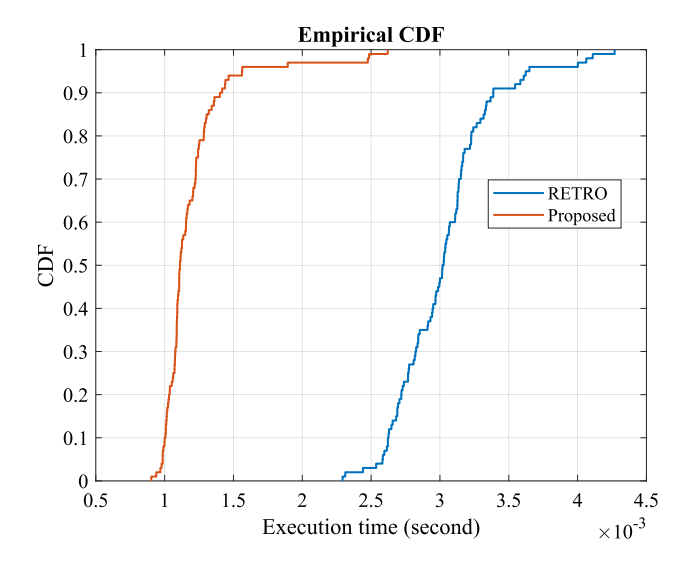


Fig. 16 A sample execution time comparison between the proposed algorithm and RETRO [10]



4.4 Investigating the time complexity

To get an estimate of the time complexity of the proposed algorithm, we perform 100 positionings measuring the execution time for each time point. Figure 14 shows a CDF plot of execution time. Clearly, in over 95% of cases, the execution time is less than 0.15 ms. The execution time with the proposed Klaman filter stage is slightly longer than the case without it. This result ensures the low time complexity and suitability of the proposed algorithm for real-time operation. These results are verified using the Matlab tic-toc command running on Matlab 2021b running on a laptop with an i5 processor and 8 GB RAM.

4.5 The impact of the regression model

In the following experiment we compare the positioning accuracy with different regression techniques. Namely, we consider SVM [22], linear [26], ensemble [27], generalized additive model (GAM) [28], Gaussian process regression (GPR) [29], and neural network regression models. We refer the interested reader to [30] for an elaborate discussion of several regression models.

Figure 15 shows the CDF plots of errors in Euclidean and angular coordinates. It is noted that SVM has the best performance compared to the others. On the other hand, the other regression techniques perform similarly. The result obtained in this experiment is intuitively expected due to the fact that the size of the dataset in this application is small compared to other application areas. Basically, one needs not have many coordinates to train an SVM model. On the other hand, SVM models are known to be particularly well-suited to complex and small datasets [31].

Finally, we compare the time complexity of the proposed algorithm to that of RETRO [10] quantified in terms of execution time. Figure 16 shows a CDF plot for each of them. It is clearly seen that the proposed algorithm has a significant saving in terms of time complexity.

5 Conclusions

In this paper, we presented an algorithm for real-time object positioning of IoT devices in indoor environments. The proposed algorithm aims at two main goals; positioning accuracy and speed. The proposed algorithm is based on exploiting the relative relationship between the power of the signal reflected from the retroreflector placed on top of the object and the set of PDs. We showed how to render this mapping using a machine-learning regression model and use it to estimate object coordinates. These models generalize well to unforeseen coordinates and

environments and excel in fast inference compared to traditional optimization-based methods. We also showed the use of Kalman filtering as a stabilizer for the estimates. Prior knowledge of previous states is used with model estimates to obtain more robust estimates. This filtering prevents abrupt changes in estimates due to errors or noise. Moreover, the proposed algorithm achieves accurate positioning performance with fast and real-time operation. These results were verified by real experiments performed on a prototype testbed.

Acknowledgements The authors gratefully acknowledge the approval and the support of this research study by Grant No. ENGA-2022-11-1649 from the Deanship of Scientific Research at Northern Border University, Arar, K.S.A.

Funding The authors gratefully acknowledge the approval and the support of this research study by grant no. ENGA-2022-11-1649 from the Deanship of Scientific Research at Northern Border University, Arar, K.S.A.

Data availability Data will be made available on request.

Declarations

Competing interests The authors declare that they have no conflict of interest.

References

- Shao, S., Khreishah, A., Ayyash, M., Rahaim, M.B., Elgala, H., Jungnickel, V., Schulz, D., Little, T.D., Hilt, J., Freund, R.: Design and analysis of a visible-light-communication enhanced wifi system. J. Opt. Commun. Netw. 7(10), 960–973 (2015)
- Do, T.-H., Yoo, M.: An in-depth survey of visible light communication based positioning systems. Sensors 16(5), 678 (2016)
- 3. Wang, Q., Zuniga, M.: Passive visible light networks: taxonomy and opportunities. In: Proceedings of the workshop on light up the IoT, pp. 42–47 (2020)
- Weiss, A.P., Rad, S.Z., Wenzl, F.P.: Pose detection with backscattered visible light sensing utilizing a single rgb photodiode: A model based feasibility study. In: 2020 international wireless communications and mobile computing (IWCMC), IEEE. pp. 137–142 (2020).
- Faulkner, N., Alam, F., Legg, M., Demidenko, S.: Watchers on the wall: passive visible light-based positioning and tracking with embedded light-sensors on the wall. IEEE Trans. Instrum. Meas. 69(5), 2522–2532 (2019)
- Lascio, E., Varshney, A., Voigt, T., Pérez-Penichet, C.: Poster abstract: Localight-a battery-free passive localization system using visible light. In: Proc. 15th ACM/IEEE Int. Conf. Inf. Process. Sensor Netw.(IPSN), pp. 1–6 (2016)
- Li, T., An, C., Tian, Z., Campbell, A.T., Zhou, X.: Human sensing using visible light communication. In: Proceedings of the 21st annual international conference on mobile computing and networking, pp. 331–344 (2015)
- Zhao, Z., Wang, J., Zhao, X., Peng, C., Guo, Q., Wu, B.: Navilight: Indoor localization and navigation under arbitrary lights. In: IEEE INFOCOM 2017-IEEE conference on computer communications, IEEE, pp. 1–9 (2017)

- Kuo, Y.-S., Pannuto, P., Hsiao, K.-J., Dutta, P.: Luxapose: indoor positioning with mobile phones and visible light. In: Proceedings of the 20th annual international conference on mobile computing and networking, pp. 447–458 (2014)
- Shao, S., Khreishah, A., Khalil, I.: Retro: Retroreflector based visible light indoor localization for real-time tracking of IoT devices. In: IEEE INFOCOM 2018-IEEE conference on computer communications, IEEE, pp. 1025–1033 (2018)
- Zhou, B., Liu, A., Lau, V.: Visible light-based user position, orientation and channel estimation using self-adaptive locationdomain grid sampling. IEEE Trans. Wirel. Commun. 19(7), 5025–5039 (2020)
- Kotaru, M., Joshi, K., Bharadia, D., Katti, S.: Spotfi: Decimeter level localization using wifi. In: Proceedings of the 2015 ACM conference on special interest group on data communication, pp. 269–282 (2015)
- Yang, S.-H., Kim, H.-S., Son, Y.-H., Han, S.-K.: Three-dimensional visible light indoor localization using AOA and RSS with multiple optical receivers. J. Lightwave Technol. 32(14), 2480–2485 (2014)
- Merzbach, U.: The mathematical papers of Isaac Newton. JSTOR (1971)
- Janik, L., Novak, M., Dobesch, A., Hudcova, L.: Retroreflective optical communication. In: 2017 conference on microwave techniques (COMITE), IEEE, pp. 1–4 (2017)
- Shao, S., Khreishah, A., Paez, J.: Passiveretro: Enabling completely passive visible light localization for iot applications. In: IEEE INFOCOM 2019-IEEE conference on computer communications, IEEE, pp. 1540–1548 (2019)
- Nazzal, M., Sawalmeh, A., Shao, S., Anan, M., Khreishah, A., Alanazi, A.: Retro-vlp: towards single light source-based realtime indoor positioning. In: 2022 13th international conference on information and communication systems (ICICS), IEEE, pp. 485–490 (2022)
- Weiss, A.P., Wenzl, F.P.: Backscattered visible light sensing of retroreflective foils utilizing random forest based classification for speed and movement direction determination and identification of an indoor moving object. In: Telecom, vol. 2, pp. 574–599. Multidisciplinary Digital Publishing Institute (2021)
- Weiss, A.P., Wenzl, F.P.: Identification and speed estimation of a moving object in an indoor application based on visible light sensing of retroreflective foils. Micromachines 12(4), 439 (2021)
- Weiss, A.P., Madane, K., Wenzl, F.P., Leitgeb, E.: Random forest based classification of retroreflective foils for visible light sensing of an indoor moving object. In: 2021 16th International conference on telecommunications (ConTEL), pp. 78–84. IEEE (2021)
- 21. Welch, G., Bishop, G., et al.: An introduction to the Kalman filter (1995)
- 22. Vapnik, V.N.: The nature of statistical learning. Theory (1995)
- Hamamtsu. https://www.hamamatsu.com/resources/pdf/ssd/ s6801 etc kpin1046e.pdf. Accessed 30 Jan 2022
- Thorlabs. https://www.thorlabs.com/newgrouppage9.cfm?ob jectgroup id=145. Accessed 30 Jan 2022
- MC. https://www.mccdaq.com/usb-data-acquisition/USB-1608FS-Plus-Series. Accessed 30 Jan 2022
- Su, X., Yan, X., Tsai, C.-L.: Linear regression. Wiley Interdiscip. Rev. 4(3), 275–294 (2012)
- Unger, D.A., van den Dool, H., Olenic, E., Collins, D.: Ensemble regression. Month. Weather Rev. 137(7), 2365–2379 (2009)
- Lou, Y., Caruana, R., Gehrke, J.: Intelligible models for classification and regression. In: Proceedings of the 18th ACM SIGKDD international conference on knowledge discovery and data mining, pp. 150–158 (2012)
- Seeger, M.: Gaussian processes for machine learning. Int. J. Neural Syst. 14(02), 69–106 (2004)



- Fahrmeir, L., Kneib, T., Lang, S., Marx, B.D.: Regression models. In: Fahrmeir, L., Kneib, T., Lang, S., Marx, B.D. (eds.) Regression, pp. 23–84. Springer, Cham (2021)
- 31. Algorithms, J.B.M.M.L.: Discover how they work and implement them from scratch. By Jason Brownlee (2016)

Publisher's Note Springer Nature remains neutral with regard to jurisdictional claims in published maps and institutional affiliations.

Springer Nature or its licensor (e.g. a society or other partner) holds exclusive rights to this article under a publishing agreement with the author(s) or other rightsholder(s); author self-archiving of the accepted manuscript version of this article is solely governed by the terms of such publishing agreement and applicable law.



include acoustic communication, wireless communications, and 4G and 5G networks using UAVs.

Ali H. Alenezi received the B.S. degree in electrical engineering from King Saud University, Saudi Arabia, the M.S. degree in electrical engineering from the Royal Institute of Technology KTH, Sweden, and the Ph.D. degree in electrical engineering from the New Jersey Institute of Technology, USA, in 2018. He is currently an Assistant Professor with the Electrical Engineering Department, Northern Border University, Saudi Arabia. His research interest



Mahmoud Nazzal (Member, IEEE) received the B.Sc. degree in electrical engineering from Birzeit University, in 2009, and the M.Sc. and Ph.D. degrees in electrical and electronic engineering from Eastern Mediterranean University, in 2010 and 2015, respectively. He was a Lecturer with the Electrical and Electronic Engineering Department, Eastern Mediterranean University, from 2015 to 2016. He was also a Lecturer with the Izmir University of Economics,

from 2016 to 2017. From July 2017 to August 2019, he was a Post-doctoral Researcher with Istanbul Medipol University. Then, he was a Lecturer with Abu Dhabi Vocational Education and Training Institute, United Arab Emirates. His research interests include sparse coding, security in machine learning, and signal processing for wireless communications.



Ahmed Sawalmeh (Member, IEEE) received the B.S. and M.S. degrees in Computer Engineering from Jordan University of Science and Technology, Jordan, in 2003 and 2006, respectively, and the Ph.D. degree in Computer and Communication Engineering from University Tenaga Nasional, Malaysia, in 2020. He is currently with Irbid National University, Jordan as an assistant professor in the Data Science and Artificial Intelligence Department at

College of Science and Information Technology. His research interests include the use of artificial intelligence and machine learning in support of wireless communications and emerging technologies for 5G and 6G networks, focusing on aerial communication networks, unmanned aerial vehicle (UAV) networks, and Flying Ad-Hoc Networks (FANETs).



Abdallah Khreishah (Senior Member, IEEE) received the B.S. degree in computer engineering from the Jordan University of Science and Technology, in 2004, and the M.S. and Ph.D. degrees in electrical and computer engineering from Purdue University, in 2006 and 2010, respectively. While pursuing his Ph.D. studies, he worked with NEESCOM. He is currently an Associate Professor with the Department of Electrical and Computer Engineering, New

Jersey Institute of Technology. His research interests include visiblelight communication, green networking, network coding, wireless networks, and network security. He is the Chair of North Jersey IEEE EMBS Chapter.



Sihua Shao [M'18] received his Ph.D. degree and the Hashimoto Prize for best doctoral dissertation from the New Jersey Institute of Technology in 2018. Currently, he is an assistant professor with the Department of Electrical Engineering at New Mexico Tech. His research interests include wireless communication and wireless networks.





Muhannad Almutiry (Member, IEEE) received the B.Sc. degree in electrical engineering from Umm Al Qura University, Mecca, Saudi Arabia, in 2007, and the M.Sc. and Ph.D. degrees in electrical engineering from the University of Dayton, Dayton, OH, USA, in 2010 and 2016, respectively. From 2013 to 2016, he was a Research Assistant at Mumma Radar Laboratory, University of Dayton. He has been an Assistant Professor with the Department

of Electrical Engineering, Northern Border University, Saudi Arabia,

since 2016. His main research interests include radar imaging, subsurface sensing, UAV detection, and sonar and intelligent adaptive radar networks.

